THE JOURNAL OF BIOLOGICAL CHEMISTRY VOL. 283, NO. 10, pp. 6594–6606, March 7, 2008

Differential Involvement of Cell Cycle Reactivation between Striatal and Cortical Neurons in Cell Death Induced by 3-Nitropropionic Acid*

Received for publication, September 14, 2007, and in revised form, December 12, 2007 Published, JBC Papers in Press, January 8, 2008, DOI 10.1074/jbc.M707730200

Hiroki Akashiba, Yuji Ikegaya, Nobuyoshi Nishiyama[1], and Norio Matsuki

From the Laboratory of Chemical Pharmacology, Graduate School of Pharmaceutical Sciences, University of Tokyo, 7-3-1 Hongo, Bunkyo-ku, Tokyo 113-0033, Japan

Recent evidence suggests that unscheduled cell cycle activity leads to neuronal cell death. 3-Nitropropionic acid (3-NP) is an irreversible inhibitor of succinate dehydrogenase and induces cell death in both striatum and cerebral cortex. Here we analyzed the involvement of aberrant cell cycle progression in 3-NP-induced cell death in these brain regions. 3-NP reduced the level of cyclin-dependent kinase inhibitor p27 in striatum but not in cerebral cortex. 3-NP also induced phosphorylation of retinoblastoma protein, a marker of cell cycle progression at late G_1 phase, only in striatum. Pharmacological experiments revealed that cyclin-dependent kinase activity and *N*-methyl-D-aspartate (NMDA) receptor were cooperatively involved in cell death by 3-NP in striatal neurons, whereas only NMDA receptor was involved in 3-NP-induced neurotoxicity in cortical neurons. Death of striatal neurons was preceded by elevation of somatic Ca^{2+} and activation of calpain, a Ca^{2+}-dependent protease. Both striatal p27 down-regulation and cell death provoked by 3-NP were dependent on calpain activity. Moreover, transfection of p27 small interfering RNA reduced striatal cell viability. In cortical neurons, however, there was no change in somatic Ca^{2+} and calpain activity by 3-NP, and calpain inhibitors were not protective. These results suggest that 3-NP induces aberrant cell cycle progression and neuronal cell death via p27 down-regulation by calpain in striatum but not in the cerebral cortex. This is the first report for differential involvement of cell cycle reactivation in different brain regions and lightens the mechanism for region-selective vulnerability in human disease, including Huntington disease.

Increasing evidence suggests that neuronal apoptosis is involved in neurodegenerative disorders (1). A greater understanding of the cellular signaling pathways that regulate neuronal apoptosis may lead to novel therapeutic targets. However, the signaling pathways are not yet fully understood.

Cell cycle progression is regulated through complex events controlled through the actions of cyclin-dependent kinases (CDKs)[2] and cyclins. In addition, two classes of CDK inhibitors are involved in cell cycle arrest mechanisms (2). Interestingly, a growing body of work shows that cell cycle components are involved in neuronal apoptotic death. For instance, neuronal apoptosis is accompanied by changes in CDK activity and cyclin expression (3–7). Moreover, agents that inhibit cell cycle progression protect neuronal PC12 cells, cortical neurons, sympathetic neurons, and cerebellar granule neurons from apoptotic death (8, 9). Similarly, overexpression of CDK inhibitors or dominant-negative CDK protect neurons from death caused by loss of trophic support (10), DNA damage (11), proteosomal inhibition (12), and ischemia (13). These results suggest that cell cycle-related molecules play pivotal roles in multiple forms of neuronal cell death.

3-Nitropropionic acid (3-NP) irreversibly inhibits mitochondrial enzyme succinate dehydrogenase and interrupts electron transport, inducing impairment of energy metabolism (reviewed in Ref. 14). Despite the mitochondrial inhibition broadly in brain (15), systemic administration of 3-NP produces selective degeneration of striatum that is reminiscent of Huntington disease (HD) (16–18). In addition, post-mortem brain extracts of HD patients showed reduced activity (19, 20) and levels of expression (21) of succinate dehydrogenase. Thus, understanding molecular machinery in 3-NP-induced selective neurodegeneration in striatum gives clues to a therapeutic strategy for HD. Although the mechanism by which 3-NP produces selective vulnerability of the striatal region is not fully understood, Galas *et al.* (22) demonstrated that calpain, a Ca^{2+}-dependent protease, is selectively activated in striatal neurons after 3-NP administration.

We previously showed that calpain activation induces cell cycle progression in glutamate-induced neurotoxicity (23). The first aim of the present study is to examine the involvement of aberrant cell cycle progression in 3-NP-induced neuronal cell death. Our results show that 3-NP treatment induced calpain activation and cell cycle activation in striatal but not in cortical neurons. Primarily cultured neurons derived from both striatum and cerebral cortex are known to be vulnerable to 3-NP (24). The second aim of the present study is to investigate the shared mechanisms of 3-NP neurotoxicity between cultured

* The costs of publication of this article were defrayed in part by the payment of page charges. This article must therefore be hereby marked "*advertisement*" in accordance with 18 U.S.C. Section 1734 solely to indicate this fact.

[1] To whom correspondence should be addressed: Laboratory of Chemical Pharmacology, Graduate School of Pharmaceutical Sciences, University of Tokyo, 7-3-1 Hongo, Bunkyo-ku, Tokyo 113-0033, Japan. Tel.: 81-3-5841-4782; Fax: 81-3-5841-4786; E-mail: nisiyama@mol.f.u-tokyo.ac.jp.

[2] The abbreviations and trivial names used are: CDK, cyclin-dependent kinase; ALLN, *N*-acetyl-Leu-Leu-Nle-aldehyde; HD, Huntington disease; Hoechst 33342, bisbenzimide *H* 33342; MDL28170, Z-Val-Phe-aldehyde; MK801 maleate, (5*R*,10*S*)-(+)-5-methyl-10,11-dihydro-5H-dibenzo[a,d]-cyclohepten-5–10-imine maleate; MSN, medium size spiny neuron; MTT, 3-(4,5-dimethylthiazol-2-yl)-2,5-diphenyltetrazolium bromide; NMDA, *N*-methyl-D-aspartate; 3-NP, 3-nitropropionic acid; OGB-1, Oregon Green 488 BAPTA-1, AM; PD150606, 3-(4-Iodophenyl)-2-mercapto-(Z)-2-propenoic acid; Rb, retinoblastoma protein; siRNA, small interfering RNA; TBS, Tris-buffered saline; Z, benzyloxycarbonyl; FMK, fluoromethyl ketone.

striatal and cortical neurons. Our results show that NMDA receptor-dependent neurotoxic mechanisms are common between neurons taken from the two regions. Thus, we here delineated both the difference and commonality in molecular machineries in 3-NP-induced death in striatal and cortical neurons.

MATERIALS AND METHODS

Primary Neuronal Culture—Primary neuronal cultures of rat striatum and cerebral cortex were prepared as described previously (25) with some modifications. All animal experiments conformed to the Japanese Pharmacological Society guide for the care and use of laboratory animals and the guidance of the University of Tokyo, with care to minimizing the number of animals and their suffering. In brief, whole brains were isolated from fetal rats of the Wistar strain (SLC Inc., Shizuoka, Japan) at embryonic days 17–18, and the striata and cerebral cortices were dissected out and treated with 0.25% trypsin (Difco) and 0.01% deoxyribonuclease I (Sigma) at 37 °C for 30 min. The cells were suspended in Neurobasal medium (Invitrogen) containing 10% fetal bovine serum (Biowest SAS, Nuaille, France). Then they were plated at a density of 1.0×10^5 cells/cm^2 in 96-well plates (Corning), in 6-well plates (Corning), in a 35-mm dish (Corning), or on glass coverslips (Matsunami Glass Ind. Ltd., Osaka, Japan) equipped with FlexiPerm (Sartorius AG, Göttingen, Germany) precoated with 0.02% (v/v) polyethyleneimine (Sigma). Cultures were kept at 37 °C in humidified 5% CO_2, 95% air. At 24 h after plating, the medium was changed to serum-free Neurobasal medium supplemented with 2% B27 (Invitrogen). Half of the culture medium was changed every 3 days.

Drug Treatment—On day 8 *in vitro*, drugs were treated by changing half of the culture medium. 3-NP (Sigma) was dissolved in water and brought to pH 7.5 with 1 N NaOH. Caspase-3-specific inhibitor, benzyloxycarbonyl-Asp-Glu-Val-Asp-fluoromethyl ketone (Z-DEVD-FMK) (Enzyme Systems Products Inc., Livermore, CA); *N*-methyl-D-aspartate (NMDA) (Sigma); three calpain inhibitors (*N*-acetyl-Leu-Leu-Nle-CHO (ALLN) (Sigma), Z-Val-Phe-CHO (MDL28170) (Merck), and 3-(4-lodophenyl)-2-mercapto-(Z)-2-propenoic acid (PD150606) (Merck)); and ubiquitin-proteasome inhibitor, lactacystin (Sigma) were added to the cell cultures simultaneously as they were treated with 3-NP. NMDA receptor antagonist (5*R*,10*S*)-(+)-5-methyl-10,11-dihydro-5H-dibenzo[a,d]-cyclohepten-5–10-imine maleate ((+)-MK801 maleate) (TOCRIS, Park Ellisville, MO) and three pharmacological CDK inhibitors (olomoucine (Sigma), purvalanol A (Merck), and roscovitine (Merck)) were added to the cell cultures 1 h prior to the treatment of 3-NP. All drugs were treated during 3-NP exposure, with continued treatment until assay.

3-NP Injection in Vivo—Male Sprague-Dawley rats (12–16 weeks old, 300–400 g) were housed at two per cage and kept under temperature- and humidity-controlled conditions (23 ± 1 °C and 50 ± 10%, respectively). 3-NP injection was conducted by two methods. In the first group, rats were injected intraperitoneally with 10 mg/kg 3-NP (Sigma; dissolved in 0.9% (w/v) saline and pH adjusted to 7.5 with 1 N NaOH) once every 4 days for 3 weeks (26). In the second group, rats were injected intraperitoneally with 7.5 mg/kg 3-NP (Sigma) twice daily for 5 days (27). In both groups, control animals received 0.9% (w/v) saline. All rats survived after 3-NP injection.

Assessment of Cell Viability—Neuronal cell viability was assessed with two methods. In the first method, cells were fixed with 4% paraformaldehyde (Wako Pure Chemical Industries, Ltd., Osaka, Japan) in phosphate-buffered saline for 30 min at 4 °C. The cells were stained and visualized with cresyl violet (Wako Pure Chemical Industries) and also identified as neurons as judged from their morphological characteristics. The number of surviving neurons was counted and normalized by setting the number of surviving neurons in nondrug control cultures as 100%. In the second method, mitochondrial dehydrogenase activity that reduces 3-(4,5-dimethylthiazol-2-yl)-2,5-diphenyltetrazolium bromide (MTT) to MTT formazan was used to determine cell survival in a quantitative colorimetric assay, a biochemical index for cellular viability (28). The cells were incubated with 0.25 mg/ml MTT (Sigma) for 35 min at 37 °C in humidified 5% CO_2, 95% air. The reaction was stopped by a solution (pH 4.7) containing 50% dimethylformamide (Wako Pure Chemical Industries) and 20% SDS (Wako Pure Chemical Industries). The amount of intracellular MTT formazan product was quantified spectrophotometrically using a microplate reader (model 550; Bio-Rad) at an excitation wavelength of 570 nm and an emission wavelength of 655 nm.

Immunocytochemistry—After fixation as described above, cells were washed and permeabilized with 0.1% Triton X-100 (Wako Pure Chemical Industries) in Tris-buffered saline (TBS) (25 mM Tris (pH 8.0), 125 mM NaCl) for 15 min. The cultures were incubated with TBS containing 5% goat serum (Vector Laboratories Inc., Burlingame, CA) for 1 h at room temperature and then with a primary antibody overnight at 4 °C. The primary antibodies used were anti-p27 (mouse, 1:200 dilution; BD Transduction Laboratories), anti-MAP2 (microtubule-associated protein-2) (rabbit, 1:1000; Chemicon International, Inc., Temecula, CA), and anti-DARPP-32 (dopamine- and cyclic AMP-regulated phosphoprotein of 32 kDa) (Santa Cruz Biotechnology, Inc., Santa Cruz, CA). After washing, the cells were incubated with a fluorochrome-conjugated secondary antibody (Alexa 488-conjugated anti-mouse or anti-goat IgG, 1:1000 dilution; Alexa 568-conjugated anti-rabbit IgG, 1:1000 dilution; Molecular Probes Inc., Eugene, OR) for 1 h at room temperature. For the last 5 min, cells were incubated with the bisbenzimide, Hoechst 33342 (Sigma), at 5 μg/ml and a fluorescent probe was intercalated into nuclear DNA. After washing, images were acquired with a cooled CCD camera (Hamamatsu ORCA II; Hamamatsu Photonics KK, Hamamatsu, Japan) and a ×40 objective lens equipped with an inverted microscope (Eclipse TE300; Nikon Corp., Tokyo, Japan). Those images were analyzed using an Aqua-Cosmos system (Hamamatsu Photonics).

Immunoblotting—In *in vitro* analysis, cells were washed with cold TBS and lysed for 30 min on ice in radioimmunoprecipitation buffer (10 mM Na_2HPO_4, 300 mM NaCl, 0.1% (w/v) SDS, 1% Nonidet P-40, 0.1% (w/v) sodium deoxycholate, 2 mM EDTA disodium salt dihydrate, pH 7.0) containing 0.5 μg/ml leupeptin (Peptide Institute Inc., Osaka, Japan), 1 μg/ml pepstatin A (Peptide Institute), 1 mM NaF (Wako Pure Chemical Industries), and 1 mM Na_3VO_4 (Wako Pure Chemical Industries). In *in vivo* analysis, brains were removed and sectioned at 400-μm

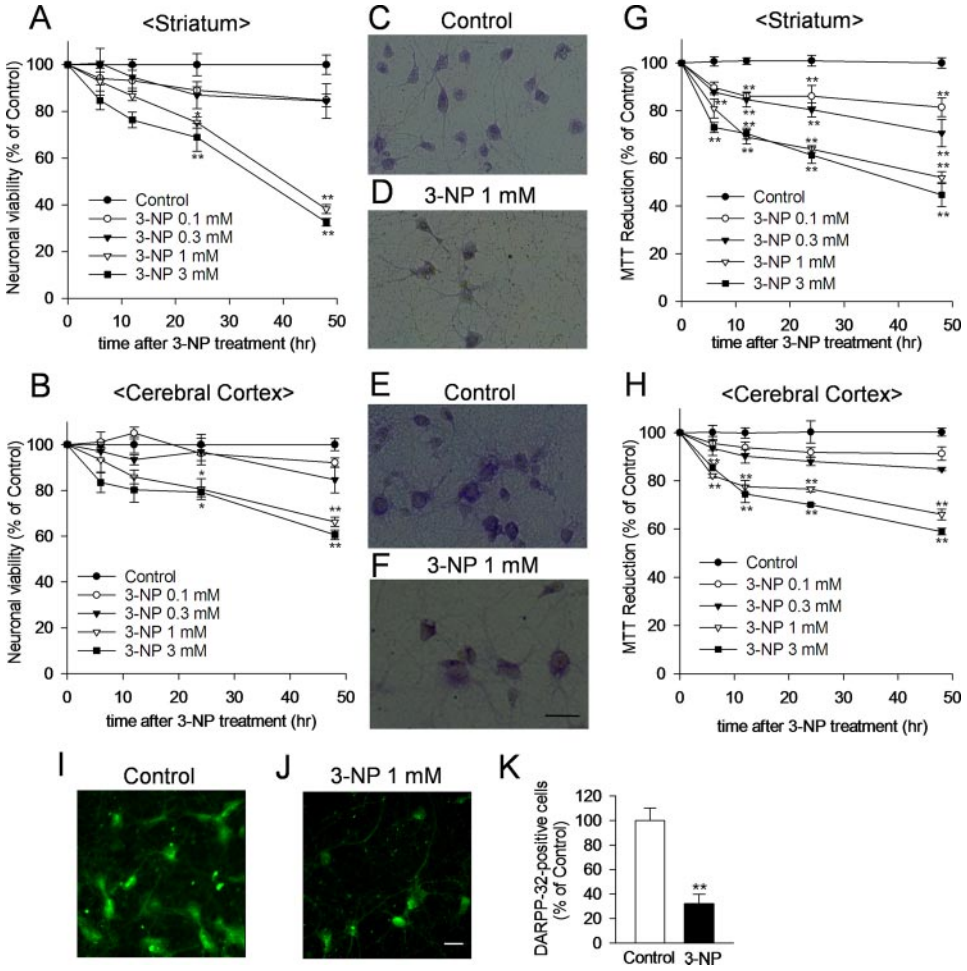

FIGURE 1. **3-NP induces neuronal cell death both in striatal and cortical neurons in a concentration- and time-dependent manner.** *A*, concentration and time dependence of 3-NP toxicity for cultured striatal neurons. Cell cultures were fixed at 6, 12, 24, and 48 h after the addition of 3-NP at the indicated concentrations and stained with cresyl violet, and the number of surviving neurons in 10 fields/well (6.46×10^4 μm^2/field) was counted. The results are presented as a percentage of control and represent the means ± S.E. of 4–5 different cultures from two independent experiments. *, $p < 0.05$; **, $p < 0.01$ *versus* control; Tukey's test. *B*, same analysis performed with cultured cortical neurons. The results are presented as a percentage of control and represent the means ± S.E. of 5–6 different cultures from two independent experiments. *, $p < 0.05$; **, $p < 0.01$ *versus* control; Tukey's test. *C–F*, representative photomicrographs of cultured striatal (*C* and *D*) and cortical (*E* and *F*) neurons stained with cresyl violet. *C* and *E*, control culture. *D* and *F*, culture exposed to 1 mM 3-NP for 48 h. *Scale bar*, 50 μm. *G*, neuronal viability was evaluated with the MTT assay at 6, 12, 24, and 48 h after the addition of 3-NP at the indicated concentrations in cultured striatal neurons. The results are presented as a percentage of control and represent the means ± S.E. of 8–12 different cultures from two independent experiments. *, $p < 0.05$; **, $p < 0.01$ *versus* control; Tukey's test. *H*, same analysis performed with cultured cortical neurons. The results are presented as a percentage of control and represent the means ± S.E. of 8–10 different cultures from two independent experiments. *, $p < 0.05$; **, $p < 0.01$ *versus* control; Tukey's test. *I* and *J*, immunoreactivity for the medium size spiny neuron marker, DARPP-32, was visualized with Alexa-488 (*green*) in cultured striatal neurons. *I*, control culture; *J*, culture exposed to 1 mM 3-NP for 48 h. *Scale bar*, 20 μm. *K*, the number of DARPP-32-positive striatal neurons in 10 fields/well (2.98×10^4 μm^2) was counted. The results are presented as a percentage of control and represent the means ± S.E. of four different cultures from two independent experiments. **, $p < 0.01$ *versus* control; Tukey's test.

thickness, and striatum and cerebral cortex were dissected under a microscope, homogenized, and lysed for 1 h on ice in radioimmunoprecipitation buffer, adding 10 mM aprotinin (Roche Applied Science) and 0.01% deoxyribonuclease I (Sigma). Proteins were denatured by heating at 65 °C in sample buffer (10 mM Tris-HCl (pH 6.8), 10 mM dithiothreitol, 2% (w/v) SDS, and 0.01% w/v bromphenol blue) for 10 min. Protein concentration was measured using a bicinchoninic acid protein assay kit according to the manufacturer's instructions (Pierce). Samples (20–50 μg) were separated electrophoretically and then transferred to polyvinylidene difluoride membranes. The membranes were blocked with 4% nonfat milk in TBS with 0.1% Tween 20 for 2 h and then incubated overnight with primary antibodies at 4 °C on a rotary platform with gentle agitation. The primary antibodies used were anti-p27 (mouse, 1:1000 dilution; BD Transduction Laboratories), anti-β-actin (mouse, 1:2000 dilution; Sigma), and anti-phosphoretinoblastoma protein (Rb) (Ser^{795}) antibody (rabbit, 1:2000 dilution; New England Biolabs, Beverly, MA). They were subsequently probed with secondary horseradish peroxidase-conjugated anti-mouse or anti-rabbit IgG antibody (diluted 1:1000–1:2000; Sigma). After washing, detection was performed using the enhanced chemiluminescence assay (Amersham Biosciences). Equal protein loading was confirmed using Coomassie Brilliant Blue staining of the gels or probing with anti-β-actin. To provide semi-quantitative analysis, band densitometry analysis of the membrane was performed using scanned images of nonsaturated immunoblot films, using software (Scion Image, version Beta 4.0.2; Scion Corp., Frederick, MD). Pixel intensities of the bands obtained in each experiment were normalized using β-actin signals and then calculated as a percentage of control bands in the same membrane.

Assessment of Calpain Activity—Assessment of calpain activity was performed by detecting the calpain-mediated breakdown products of α-spectrin in immunoblotting. Cell lysates were prepared as described above; samples were processed for gel electrophoresis and blotting. The primary antibody used was anti-α-spectrin (mouse, 1:1000 dilution; Chemicon). (Pixel intensity × area of 145-kDa α-spectrin breakdown product)/(pixel intensity × area of (145-, 150-, and 280-kDa α-spectrin)) was measured densitometrically using software (Scion Image, version Beta 4.0.2; Scion Corp.). The individual band density was calculated as a percentage of control signals.

In Vitro Degradation of p27 with Purified Calpain—On days 7–8 *in vitro*, striatal cells were washed with cold TBS and then lysed for 30 min on ice in radioimmunoprecipitation buffer containing 1 μg/ml pepstatin A (Peptide Institute), 1 mM NaF (Wako Pure Chemical Industries), and 1 mM Na_3VO_4 (Wako

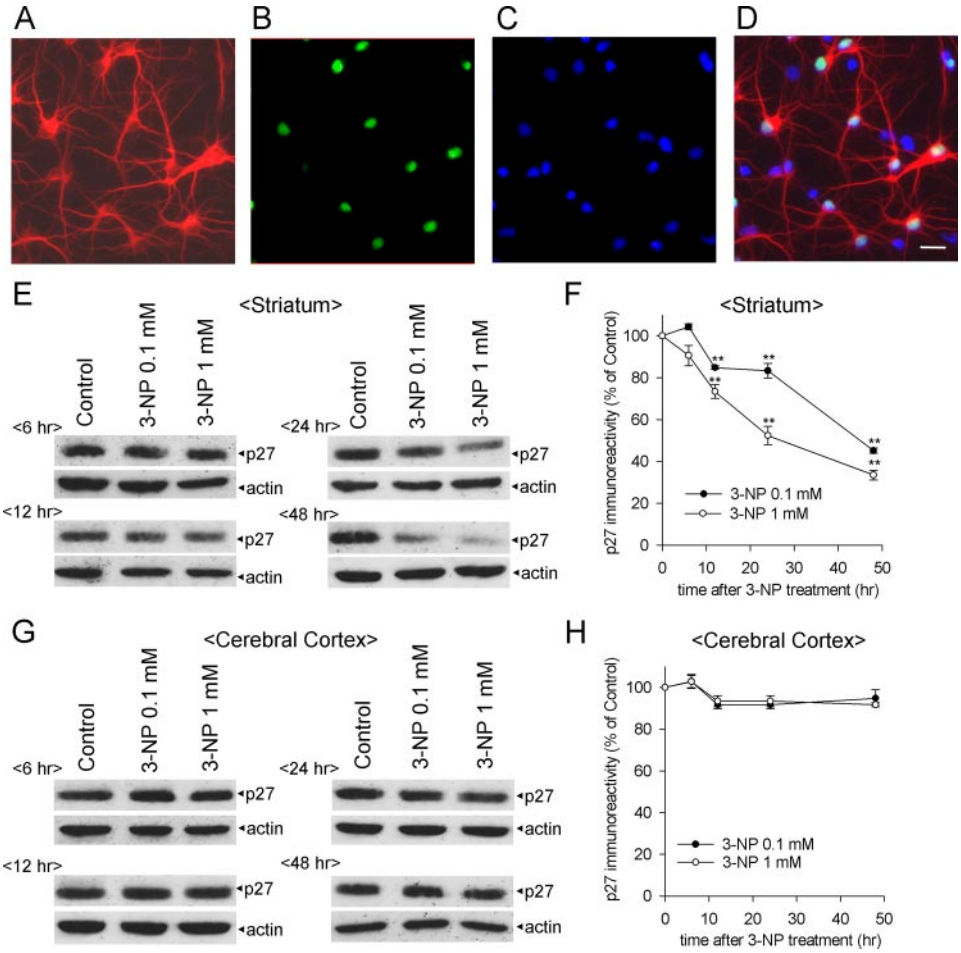

FIGURE 2. **3-NP decreases p27 expression in striatal but not in cortical neurons.** *A–D*, immunoreactivity for the neuronal marker, MAP2, was visualized with Alexa-568 (*red*) (*A*); p27 was visualized with Alexa-488 (*green*) (*B*). *Blue* represents the nucleus stained with Hoechst dye (*C*). Triple labeling for MAP2, p27, and Hoechst dye showed that p27 was expressed exclusively in the nucleus of cultured striatal neurons under control conditions (*D*). *Scale bar*, 20 μm. *E*, representative immunoblots of p27 at 6, 12, 24, and 48 h after the addition of 3-NP at the indicated concentrations in cultured striatal neurons. The expression level of p27 was down-regulated concentration- and time-dependently by 3-NP. Actin served as an internal control. *F*, the pixel intensity of the striatal p27 bands obtained in each experiment was calculated as described under "Materials and Methods." The results are presented as a percentage of control and represent the means ± S.E. of three or four different cultures from three independent experiments. **, $p < 0.01$ *versus* control; Tukey's test. *G*, representative immunoblots of p27 at 6, 12, 24, and 48 h after the addition of 3-NP at the indicated concentrations in cultured cortical neurons. The expression level of p27 was unchanged after 3-NP treatment. Actin served as an internal control. *H*, the pixel intensity of the cortical p27 bands obtained in each experiment was calculated as described under "Materials and Methods." The results are presented as a percentage of control and represent the means ± S.E. of three different cultures from three independent experiments.

Pure Chemical Industries). Calpain inhibitors (ALLN, MDL28170, and PD150606) or ubiquitin-proteasome inhibitor (lactacystin) were included in the radioimmunoprecipitation buffer. The cell lysates were incubated with 3.8 units/ml of calpain 1 (Merck) at 25 °C for 10 min. Calcium chloride dihydrate (10 μM) was added to the reaction mixture to increase the free Ca^{2+} concentration. After the reaction, sample buffer was added. The samples were processed for gel electrophoresis and immunoblotting. Control experiments verified that the addition of $CaCl_2$ to the radioimmunoprecipitation buffer over the range used in this study did not measurably alter the buffer pH.

Small Interfering RNA (siRNA) Preparation and Transfection—siRNAs were prepared and transfected as previously described (29). siRNAs were synthesized by Qiagen (Hilden, Germany). The target sequences were as follows. Control siRNA was 5′-AATTCTCCGAACGTGTCACGT-3′. The 3′-sense strand was labeled with Alexa Fluor-488. Scrambled p27 siRNA was 5′-AAGACCGAGCCATTGAGGTAA-3′. p27 siRNA was 5′-AAGCACUGCCGAGAUAUGGAA-3′. Transfection was performed with Lipofectamine 2000 (Invitrogen). Briefly, Lipofectamine 2000 (5 μl/well) and siRNA (5 μl/well) were incubated at 25 °C for 5 min, and both were mixed at 25 °C for 20 min. The siRNA-lipid mixture was added to the cultures. The final amount of the siRNAs was 100 pmol/well. siRNA was removed by changing the medium at 4 h after the transfection.

Ca^{2+} Imaging—On day 8 *in vitro*, cells in a 35-mm dish were filled with 2 ml of dye solution and incubated for 1 h in a humidified incubator at 37 °C in 5% CO_2, 95% air as previously described (30). The dye solution was Neurobasal medium (Invitrogen) containing 10 μl of 0.1% Oregon Green 488 BAPTA-1, AM (OGB-1; Invitrogen)/Me_2SO. Images (16-bit intensity) were captured with a Nipkow-disk confocal unit (CSU10; Yokogawa Electric, Tokyo, Japan), a cooled CCD camera (Cascade 512B/F, Roper Scientific, Tucson, AZ), an upright microscope (AxioSkop2; Zeiss, Oberkochen, Germany), water immersion objective (×40, Achroplan; Zeiss), and MetaMorph software (Molecular Devices, Union City, CA). Fluorophores were excited at 488 nm with an argon-krypton laser (15 milliwatts, 641-YB-A01; Melles Griot, Carlsbad, CA) and visualized with a 507-nm long pass emission filter. For quantitative analysis, OGB-1 fluorescence intensity in the soma area of each neuron (data in nonneuronal cells were excluded by phase-contrast image) were measured using software (Image J, version 1.371.20; Microsoft Java, Redmond, WA) and then calculated as a percentage of control in nontreated cultures.

Statistical Evaluation—Data are shown as mean ± S.E. To avoid possible variation of the cell cultures, data were pooled from at least two independent experiments. For statistical analyses, one-way analysis of variance was followed by Tukey's test.

RESULTS

3-NP Induces Cell Death both in Cultured Striatal and Cortical Neurons—3-NP treatment of cultured striatal cells resulted in concentration- and time-dependent reduction in

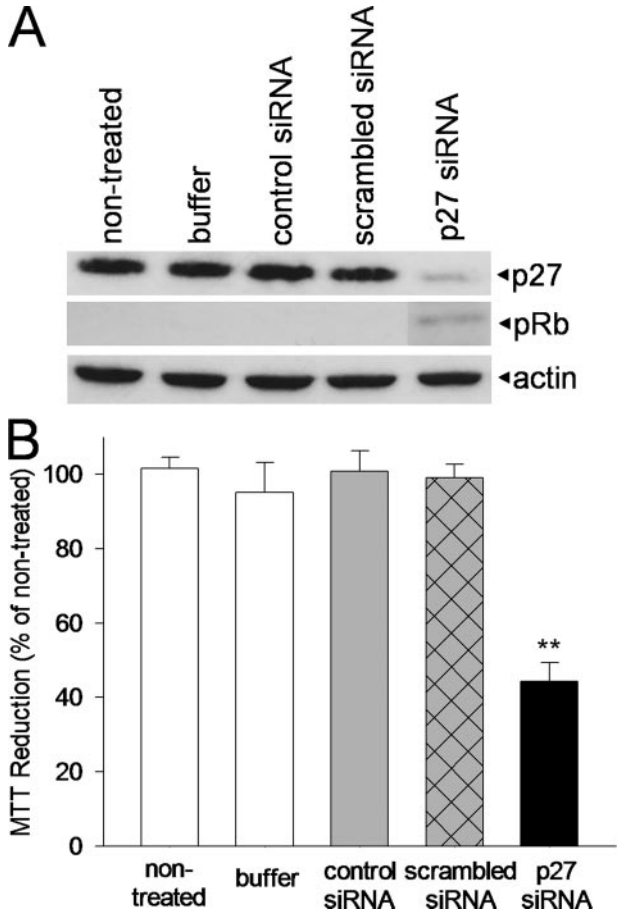

FIGURE 3. **Transfection of p27 siRNA induces reduction of p27, Rb phosphorylation, and neuronal cell death in cultured striatal neurons.** *A*, representative immunoblots of p27 and phospho-Rb (*pRb*) at 48 h after transfection of (from *left*) nontransfected control (nontreated), buffer to dilute siRNA, control siRNA, scrambled siRNA, and p27 siRNA (each 100 pmol/well). Actin served as an internal control. Similar results were obtained in three different cultures from three independent experiments. *B*, neuronal viability was evaluated with the MTT assay at 48 h after the transfection. The results are presented as a percentage of nontreated cells and represent the means ± S.E. of three or four different cultures from three independent experiments. **, $p <$ 0.01 *versus* nontreated; Tukey's test.

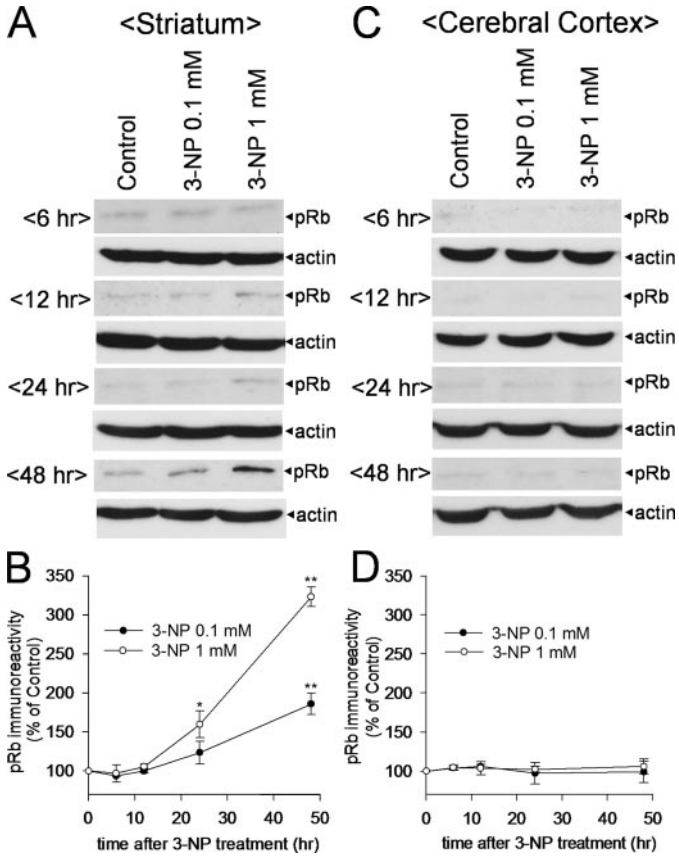

FIGURE 4. **3-NP induces Rb phosphorylation in striatal but not in cortical neurons.** *A*, representative immunoblots of phospho-Rb (*pRb*) at 6, 12, 24, and 48 h after the addition of 3-NP at the indicated concentrations in cultured striatal neurons. The expression level of phospho-Rb was up-regulated concentration- and time-dependently by 3-NP. Actin served as an internal control. *B*, the pixel intensity of the striatal phospho-Rb bands obtained in each experiment was calculated as described under "Materials and Methods." The results are presented as a percentage of control and represent the means ± S.E. of three different cultures from three independent experiments. *, $p < 0.05$; **, $p < 0.01$ *versus* control; Tukey's test. *C*, representative immunoblots of phospho-Rb at 6, 12, 24, and 48 h after the addition of 3-NP at the indicated concentrations in cultured cortical neurons. The expression level of phospho-Rb was unchanged by 3-NP. Actin served as an internal control. *D*, the pixel intensity of the cortical phospho-Rb bands obtained in each experiment was calculated as described under "Materials and Methods." The results are presented as a percentage of control and represent the means ± S.E. of three or four different cultures from three independent experiments.

the number of surviving neurons, as observed in cresyl violet (Nissl) staining (Fig. 1*A*). 3-NP did not affect neuronal viability at 0.1 and 0.3 mM, but marked cell death was apparent in cultures treated with 3-NP at concentrations as low as 1 mM (Fig. 1*A*). In the presence of 1 and 3 mM 3-NP, about 60 and 70% of total neurons degenerated at 48 h, respectively. Similarly, exposure of cortical neurons to 3-NP resulted in concentration- and time-dependent reduction in the number of surviving neurons (Fig. 1*B*). 3-NP did not show toxic effect at 0.1 and 0.3 mM, but marked cell death was apparent in cultures treated with 3-NP at more than 1 mM (Fig. 1*B*). In the presence of 1 and 3 mM 3-NP, about 30 and 40% of total cortical neurons degenerated at 48 h, respectively. In both striatal and cortical cultures, the surviving neurons, as judged from the cresyl violet-positive staining, displayed deformed morphology (Fig. 1, *C–F*).

We also evaluated cell survival by MTT assay. The results obtained with this method showed concentration- and time-dependent toxicity of 3-NP both in cultured striatal and cortical neurons, which were almost identical with the results of the cresyl violet staining method (Fig. 1, *G* and *H*). Because the two methods gave similar results, the following experiments to assess neuronal viability were performed with MTT assay.

Next we examined whether striatal neurons sensitive to 3-NP were medium size spiny neurons (MSNs). We performed immunocytochemical analysis using labeling for DARPP-32, a molecule enriched in MSNs (31). Under control conditions, about 90% of striatal neurons were DARPP-32-positive in our experiment (data not shown). In cultures exposed to 3-NP (1 mM) for 48 h, the number of DARPP-32-positive cells decreased by about 30% compared with nontreated controls (Fig. 1, *I–K*).

3-NP Decreases p27 Expression in Cultured Striatal but Not in Cortical Neurons—Our previous work suggests that among CDK inhibitors involved in cell cycle arrest, p27 plays a critical role in regulation of cell cycle progression and neuronal survival (29). Immunocytochemical analysis using triple labeling for a neuronal marker MAP2, p27, and a nuclear marker Hoechst

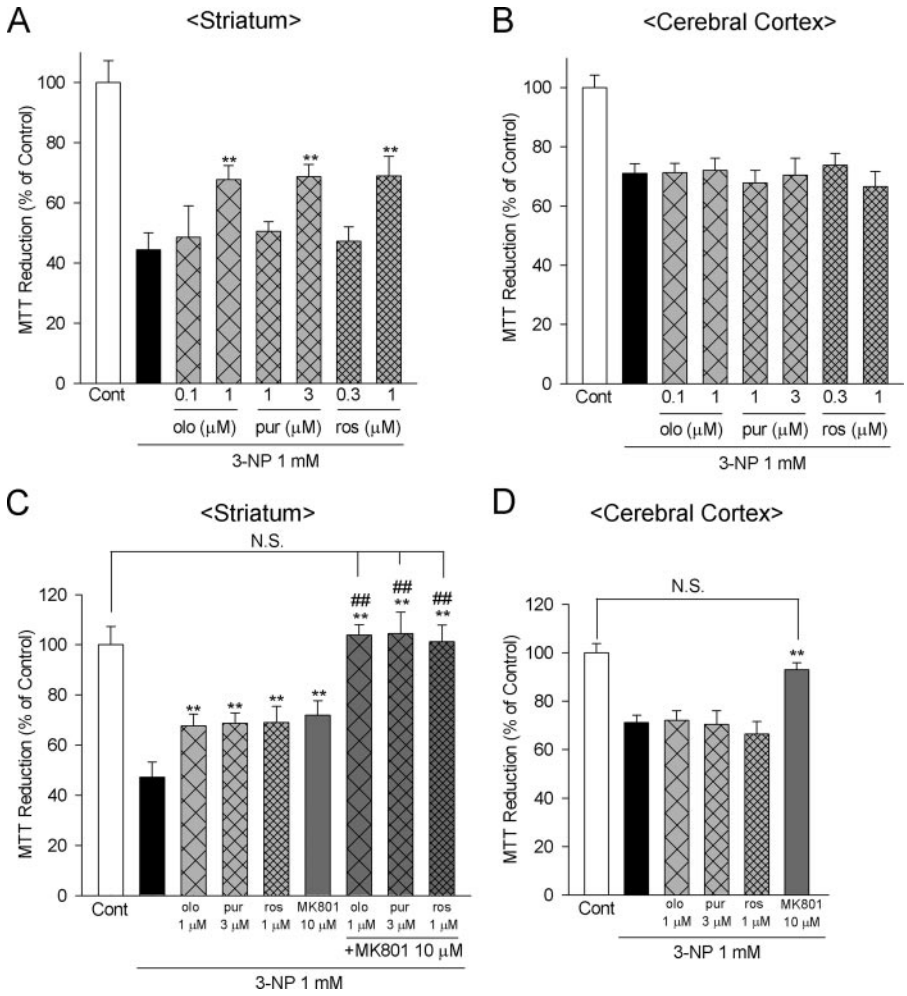

FIGURE 5. **CDK and NMDA receptor activities are involved in the 3-NP-induced cell death in striatal neurons, whereas NMDA receptor activity is involved in cell death by 3-NP in cortical neurons.** All drugs were treated 1 h prior to the addition of 3-NP, with continued treatment until assay. *A*, pharmacological CDK inhibitors, olomoucine (*olo*), purvalanol A (*pur*), and roscovitine (*ros*), protected from 3-NP-induced cell death in cultured striatal neurons. Neuronal viability was evaluated with the MTT assay at 48 h after 3-NP treatment. The results are presented as a percentage of control and represent the means ± S.E. of 10–12 different cultures from three independent experiments. *Cont*, control. **, $p < 0.01$ *versus* 3-NP; Tukey's test. *B*, pharmacological CDK inhibitors, olomoucine, purvalanol A, and roscovitine, did not protect from the 3-NP-induced cell death in cultured cortical neurons. Neuronal viability was evaluated with the MTT assay at 48 h after 3-NP treatment. The results are presented as a percentage of control and represent the means ± S.E. of 9–15 different cultures from three independent experiments. *Cont*, control. *C*, co-treatment of CDK inhibitors and NMDA receptor blocker (MK801) protected from cell death by 3-NP almost completely in cultured striatal neurons. Neuronal viability was evaluated with the MTT assay at 48 h after 3-NP treatment. The results are presented as a percentage of control and represent the means ± S.E. of 10–15 different cultures from three independent experiments. *Cont*, control. *N.S.*, not significant. **, $p < 0.01$ *versus* 3-NP. ##, $p < 0.01$ *versus* CDK inhibitor or MK801 alone; Tukey's test. *D*, NMDA receptor blocker (MK801) protected from the 3-NP-induced cell death in cultured cortical neurons. Neuronal viability was evaluated with the MTT assay at 48 h after 3-NP treatment. The results are presented as a percentage of control and represent the means ± S.E. of 8–10 different cultures from two independent experiments. *Cont*, control. *N.S.*, not significant. **, $p < 0.01$ *versus* 3-NP; Tukey's test.

dye revealed that p27 is localized in the nucleus of striatal neurons under control conditions (Fig. 2, *A–D*). This pattern of p27 expression in cultured striatal neurons is similar to that in cultured cortical neurons, as shown in our previous research (23). Next, we analyzed the p27 expression after 3-NP treatment in both cultures with an immunoblotting method. 3-NP treatment decreased the expression level of p27 concentration- and time-dependently in striatal neurons (Fig. 2, *E* and *F*). However, p27 expression in cortical neurons was unchanged by 3-NP treatment at all concentrations and times examined (Fig. 2, *G* and *H*).

Transfection of p27 siRNA Induces Cell Death in Cultured Striatal Neurons—We previously showed that transfection of p27 siRNA induced cell death through elevating cell cycle activity in cultured cortical neurons, suggesting that reduction of endogenous p27 is sufficient for cell death in cortical neurons (29). The same p27 siRNA was transfected to cultured striatal neurons to examine its effect on cell cycle progression and cell viability. The expression level of p27 was decreased at 48 h after the transfection of p27 siRNA at 100 pmol/well, whereas control siRNA or scrambled p27 siRNA had no effect on p27 expression (Fig. 3*A*). When the cell cycle transits from G_1 to S phase, tumor suppressor Rb is phosphorylated by CDKs (32). To examine whether reduction of p27 is critical for cell cycle progression, we analyzed the Rb phosphorylation status on a CDK consensus site, Ser-795, by p27 knockdown. Transfection of p27 siRNA increased the expression level of phosphorylated Rb at 48 h after transfection, whereas control siRNA or scrambled p27 siRNA had no effect on Rb phosphorylation (Fig. 3*A*). p27 siRNA reduced striatal neuronal viability at about 55% at 48 h after the transfection, whereas control siRNA or scrambled p27 siRNA did not affect the viability of striatal neurons (Fig. 3*B*).

3-NP Induces Rb Phosphorylation in Cultured Striatal but Not in Cortical Neurons—Next, we analyzed the Rb phosphorylation status after 3-NP treatment using the phosphoepitope antibody in cultured striatal and cortical neurons. Only a trace level of phosphorylated Rb immunoreactivity was detected in nontreated cultures from both regions (Fig. 4, *A–D*). The expression level of phosphorylated Rb was up-regulated concentration- and time-dependently after 3-NP treatment in striatal neurons (Fig. 4, *A* and *B*). On the other hand, expression level of phosphorylated Rb did not increase after 3-NP treatment in cortical neurons at all concentrations and times examined (Fig. 4, *C* and *D*).

CDK and NMDA Receptor Activities Are Cooperatively Involved in 3-NP-induced Cell Death in Cultured Striatal Neurons, whereas Only NMDA Receptor Activity Is Involved in 3-NP-induced Cell Death in Cultured Cortical Neurons—We next examined whether CDK activity is involved in the 3-NP-

induced cell death in striatal and cortical cultures with pharmacological experiments. Three pharmacological CDK inhibitors, olomoucine (0.1–1 μM), purvalanol A (1–3 μM), and roscovitine (0.3–1 μM), partially but significantly protected striatal neurons from 3-NP-induced cell death (Fig. 5*A*). These pharmacological CDK inhibitors, however, did not exert a protective effect against 3-NP toxicity in cortical neurons (Fig. 5*B*). 3-NP-induced blockade of ATP production may hamper sodium-potassium-ATPase pumps and lead to reduced plasma membrane potentials (33). This would produce relief of voltage-dependent Mg^{2+} blockade of NMDA receptors and cause its overactivation. Thus, we examined the effect of co-treatment of CDK inhibitors and NMDA receptor antagonist MK801. Singular treatment of MK801 (10 μM) exerted partial neuroprotective effect against 3-NP toxicity in striatal neurons (Fig. 5*C*). The effect of MK801 was maximal at this concentration (data not shown). Co-treatment of olomoucine (1 μM), purvalanol A (3 μM), and roscovitine (1 μM) and noncompetitive NMDA receptor antagonist MK801 (10 μM) protected striatal neurons from 3-NP-induced neurotoxicity almost completely (Fig. 5*C*). In cortical neurons, singular treatment with MK801 (10 μM) protected neurons almost completely from cell death induced by 3-NP treatment (Fig. 5*D*).

3-NP Induces Calpain Activation in Cultured Striatal but Not in Cortical Neurons—Previous reports demonstrate that Ca^{2+}-activated neutral protease calpain plays an important role in 3-NP-induced neurotoxicity in striatum (34). Thus, we analyzed enzymatic activity of calpain in striatal and cortical neurons after 3-NP treatment under our experimental conditions. We evaluated calpain-like activity from the expression level of the 145-kDa fragment of cytoskeletal protein α-spectrin as described previously (23). The calpain-like activity elevated from 1 h peaked to 2.5-fold at 3 h after 3-NP treatment in striatal neurons (Fig. 6, *A* and *B*). However, the calpain-like activity did not increase after 3-NP treatment in cortical neurons at all times examined (Fig. 6, *C* and *D*). Although calpain activity is mainly regulated by intracellular Ca^{2+}, this elevation of calpain-like activity by 3-NP in striatal neurons was not abrogated by MK801 (*i.e.* under blockade of NMDA receptor with high Ca^{2+} permeability) (data not shown).

Calpain-dependent Reduction of p27 by 3-NP in Cultured Striatal Neurons—Next, we examined the molecular mechanism of elevated cell cycle activity by 3-NP treatment in striatal neurons. Our previous research suggests that calpain activation is required for cell cycle progression through p27 down-regulation in glutamate-induced neurotoxicity (23). Thus, we raised a hypothesis that calpain activation by 3-NP, which is region-specific for striatal neurons, induces reduction of p27 with striatum predominance (Fig. 2). Three calpain inhibitors, ALLN (1 μM), MDL28710 (1 μM), and PD150606 (1 μM), abrogated the decrease in p27 by 3-NP treatment in striatal neurons almost completely (Fig. 7, *A* and *B*). However, lactacystin, an inhibitor of the ubiquitin-proteasome pathway, which is a main regulator of p27 expression in proliferating cells (35), did not suppress p27 down-regulation by 3-NP in striatal neurons (Fig. 7, *A* and *B*).

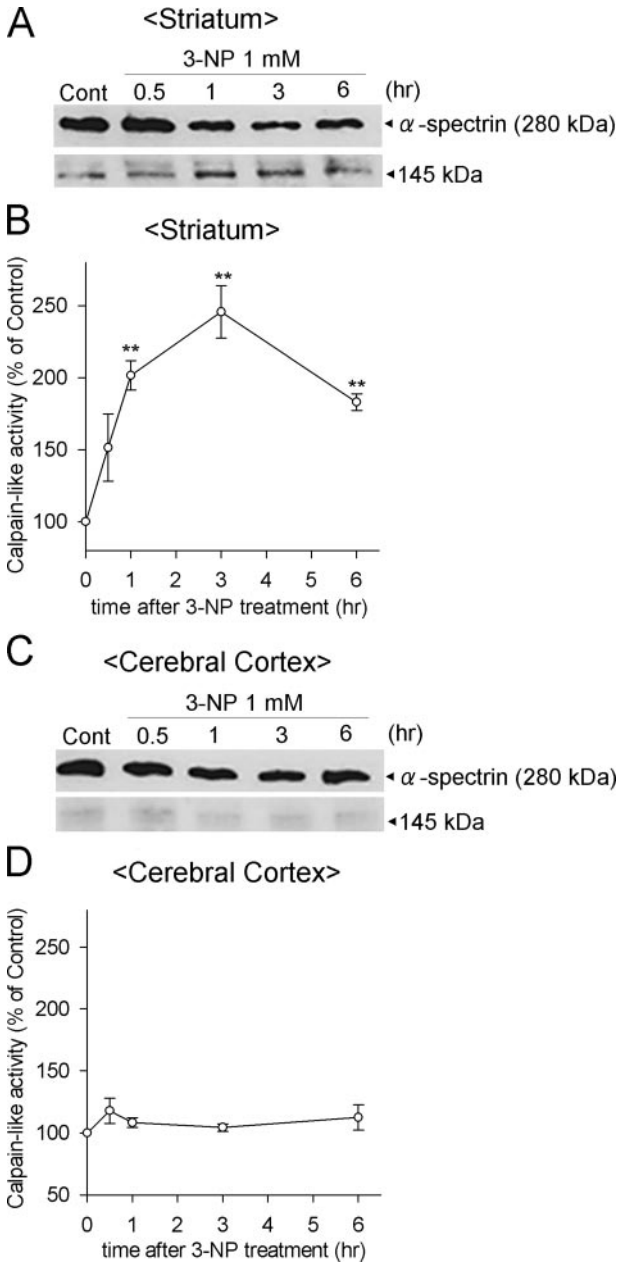

FIGURE 6. **3-NP induces calpain activation in striatal but not in cortical neurons.** *A*, representative immunoblots of α-spectrin at 0.5, 1, 3, and 6 h after the addition of 3-NP in cultured striatal neurons. The expression level of α-spectrin breakdown product at 145 kDa was up-regulated after 3-NP treatment. *Cont*, control. *B*, time course of calpain-like activity in cultured striatal neurons exposed to 1 mM 3-NP. The calpain-like activity was calculated as the changes in the 145-kDa α-spectrin fragment as described under "Materials and Methods." The results are presented as a percentage of control and represent the means ± S.E. of three or four different cultures from three independent experiments. **, $p < 0.01$ *versus* control; Tukey's test. *C*, representative immunoblots of α-spectrin at 0.5, 1, 3, and 6 h after the addition of 3-NP in cultured cortical neurons. The expression level of α-spectrin breakdown product at 145 kDa was unchanged after 3-NP treatment. *Cont*, control. *D*, time course of calpain-like activity in cultured cortical neurons exposed to 1 mM 3-NP. The calpain-like activity was calculated as the changes in the 145-kDa α-spectrin fragment as described under "Materials and Methods." The results are presented as a percentage of control and represent the means ± S.E. of three different cultures from three independent experiments.

Next we incubated neuronal cell lysate with calpain to reveal whether p27 is directly degraded for activated calpain. Among the 14 superfamilies of calpain (36), we examined

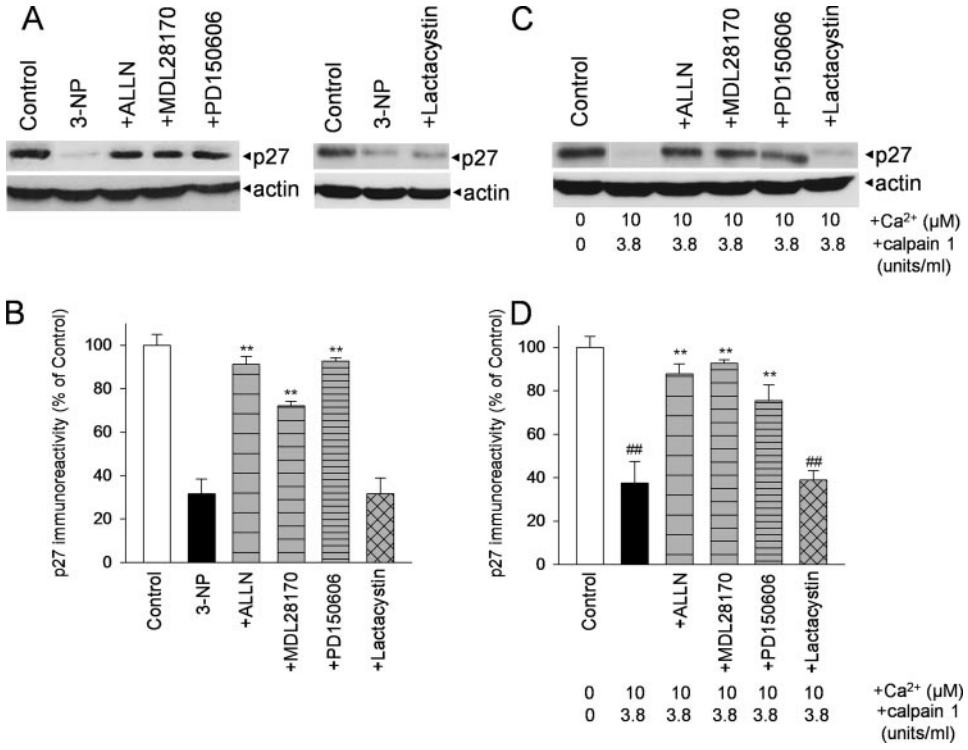

FIGURE 7. **Calpain-dependent reduction of p27 after 3-NP treatment in cultured striatal neurons.** All drugs were treated simultaneously as they were treated with 3-NP, with continuous treatment until assay. *A*, representative immunoblots of p27 at 48 h after the addition of 1 mM 3-NP in cultured striatal neurons. The p27 down-regulation by 3-NP was abrogated by calpain inhibitors, ALLN (1 μM), MDL28170 (1 μM), and PD150606 (1 μM), but not by ubiquitin-proteasome inhibitor, lactacystin (5 μM). Actin served as an internal control. *B*, the pixel intensity of the striatal p27 bands obtained in each experiment was calculated as described under "Materials and Methods." The results are presented as a percentage of control and represent the means ± S.E. of three or four different cultures from two independent experiments. **, $p < 0.01$ *versus* 3-NP; Tukey's test. *C*, cell lysates from striatal neurons were incubated with calpain 1 (3.8 units/ml) and Ca^{2+} (10 μM). Samples were subjected to gel electrophoresis and immunoblot analyses. The amount of p27 in the lysates was decreased in the presence of calpain 1 and Ca^{2+}. Calpain inhibitors, ALLN (1 μM), MDL28170 (1 μM), and PD150606 (1 μM), but not ubiquitin-proteasome inhibitor, lactacystin (5 μM), abrogated the degradation of p27. *D*, the pixel intensity of the striatal p27 bands obtained in each experiment was calculated as described under "Materials and Methods." The results are presented as a percentage of control and represent the means ± S.E. of three different cultures from two independent experiments. ##, $p < 0.01$ *versus* control; **, $p < 0.01$ *versus* 3-NP; Tukey's test.

major calpain isozyme, calpain 1, which is highly expressed in neurons (23, 37) and requires approximately 1–10 μM Ca^{2+} for activity *in vitro* (38). The amount of p27 in the lysate of striatal neurons was decreased by incubation with calpain 1 (3.8 units/ml) and $CaCl_2$ (10 μM). The calpain inhibitors, ALLN (1 μM), MDL28170 (1 μM), and PD150606 (1 μM), but not the ubiquitin-proteasome inhibitor, lactacystin (5 μM), suppressed p27 degradation incubated with calpain 1 (Fig. 7, *C* and *D*). These results suggest that calpain activation is causally associated with 3-NP-induced reduction of p27 in striatal neurons.

Calpain Activation Is Involved in 3-NP-induced Cultured Striatal Cell Death—We next examined whether calpain activation is required for cell death by 3-NP in striatal and cortical neurons. As described in the legend to Fig. 1, 3-NP treatment (1 mM) decreased neuronal viability by ~55% in striatal neurons and by ~30% in cortical neurons in 48 h as assessed with an MTT assay. Three calpain inhibitors, ALLN (0.1–1 μM), MDL28170 (0.1–1 μM), and PD150606 (0.1–1 μM), protected striatal neurons against the 3-NP neurotoxicity by about 30–35% (Fig. 8*A*). However, these calpain inhibitors had no protective effect on 3-NP neurotoxicity in cortical neurons at all concentrations examined (Fig. 8*B*). Next, we examined whether caspase-3, which plays an important role in neuronal apoptosis (39, 40), is involved in neuronal cell death by 3-NP. In both striatal and cortical cultures, caspase-3-specific inhibitor, Z-DEVD-FMK, did not exert a neuroprotective effect. Treatment of each inhibitor alone had no effect on the neuronal viability in both cultures (data not shown).

3-NP Induces an Elevation of Somatic Ca^{2+} Concentrations in Cultured Striatal but Not in Cortical Neurons—We questioned why calpain (and presumably the cell cycle pathway) is activated in striatal neurons but not in cortical neurons. Since calpain activity is regulated mainly by intracellular Ca^{2+}, we carried out functional Ca^{2+} imaging in striatal and cortical neurons using the Ca^{2+} indicator OGB-1. In both cultures, weak OGB-1 fluorescence was observed in the soma area of each neuron under basal conditions (Fig. 9, *A* and *E*). In striatal neurons, the fluorescence did not change in intensity at 30 min after 3-NP treatment (Fig. 9*C*), but after 1 h, it increased to ~150%, compared with control (Fig. 9, *A–C*) and returned to the base-line level after 4 h (Fig. 9*C*). In contrast, in cortical neurons, 3-NP treatment failed to induce an increase in OGB-1 fluorescence at any time points examined (Fig. 9, *E–G*).

Next we performed pharmacological experiments to investigate the mechanism of the region-specific somatic Ca^{2+} increase. The noncompetitive NMDA receptor antagonist MK801 (10 μM) did not block the elevation of somatic OGB-1 fluorescence at 1 h after 3-NP treatment in striatal neurons (Fig. 9*D*); nor did MK801 have an effect in cortical neurons (Fig. 9*H*). In both cultures, NMDA (10 μM) induced a ~180% increase in OGB-1 fluorescence intensity, which was almost completely blocked by 10 μM MK801 (Fig. 9, *D* and *H*).

3-NP Induces Striatum-specific Cell Cycle Progression in Vivo—Finally, we investigated whether our results *in vitro* were reproduced *in vivo* model by 3-NP injection. 3-NP injection was conducted with two protocols as described under "Materials and Methods": (i) 10 mg/kg 3-NP injection intraperitoneally once every 4 days for 3 weeks; (ii) 7.5 mg/kg 3-NP injection intraperitoneally twice daily for 5 days. In both protocols, in striatum, the expression level of p27 was down-regulated by 3-NP injec-

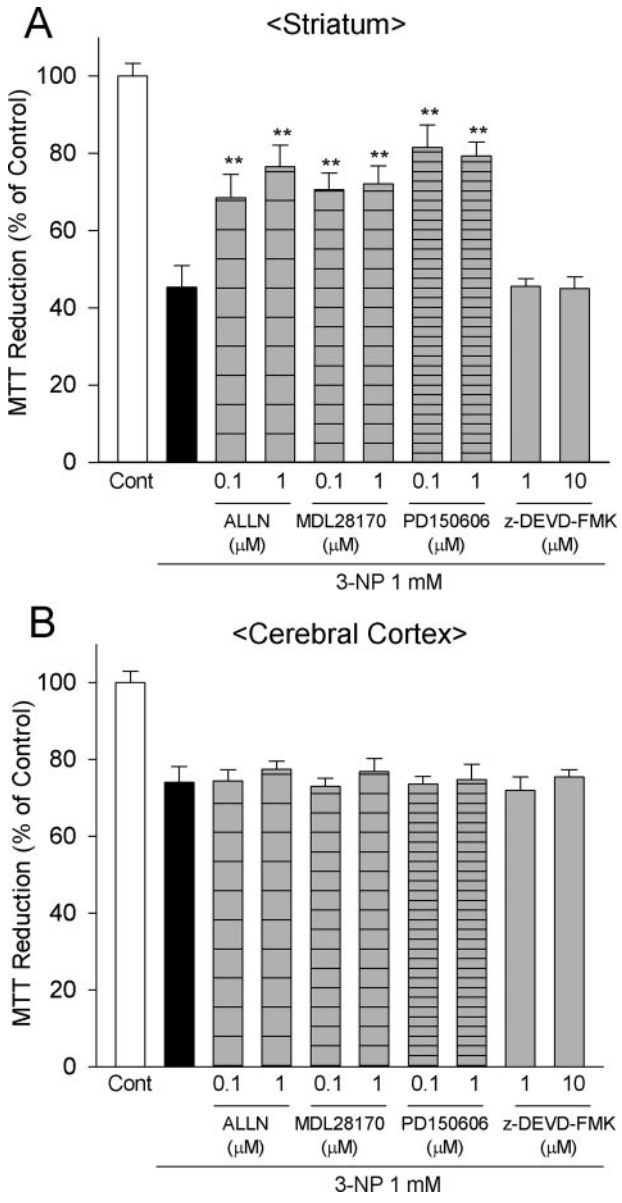

FIGURE 8. **Calpain activation is involved in the 3-NP-induced cell death in striatal, not in cortical, neurons.** All drugs were treated simultaneously as they were treated with 3-NP, with continuous treatment until assay. *A*, calpain inhibitors (ALLN, MDL28170, and PD150606) but not caspase-3 inhibitor (Z-DEVD-FMK) protected from the 3-NP-induced cell death in cultured striatal neurons. Neuronal viability was evaluated with the MTT assay at 48 h after 3-NP treatment. The results are presented as a percentage of control and represent the means ± S.E. of 10–12 different cultures from two independent experiments. *Cont*, control. **, $p < 0.01$ *versus* 3-NP; Tukey's test. *B*, calpain inhibitors (ALLN, MDL28170, and PD150606) and caspase-3 inhibitor (Z-DEVD-FMK) did not protect from the 3-NP-induced cell death in cultured cortical neurons. Neuronal viability was evaluated with the MTT assay at 48 h after 3-NP treatment. The results are presented as a percentage of control and represent the means ± S.E. of 8–10 different cultures from three independent experiments. *Cont*, control.

tion (Fig. 10, *A* and *B*). Moreover, 3-NP injection increased expression level of phosphorylated Rb in striatum (Fig. 10, *A* and *C*). In contrast, in cerebral cortex, there was no change in expression levels of p27 and phosphorylated Rb by 3-NP injection (Fig. 10, *D–F*).

DISCUSSION

In the present study, we revealed distinct mechanisms of 3-NP neurotoxicity: both cell cycle reactivation via calpain-mediated p27 down-regulation and NMDA receptor involvement in striatum but only NMDA receptor involvement in cerebral cortex.

Neuronal cell death induced by 3-NP has been investigated in multiple experimental systems. Chronic administration of 3-NP produces lesions primarily in the striatum (16, 26, 41, 42, 43). Despite its selective toxicity affecting striatum *in vivo*, 3-NP induced cell death in cultured striatal and cortical neurons in our experimental system. Consistent with our data, others reported that cultured striatal, cortical, and hippocampal neurons are sensitive to 3-NP (24, 44). Lack of organized glutamatergic input in dispersedly cultured neurons may explain the nonselectivity of 3-NP toxicity *in vitro* (45). In addition, removing dopaminergic or glutamatergic afferents by decortication suppresses striatal vulnerability to 3-NP *in vivo* (16). Altogether, our results and the results of others suggest that 3-NP has neurotoxicity on cultured neurons regardless of the regions they were derived.

MSN is the primary projection neuron of the striatum and accounts for over 95% of the striatal neurons (46). Consistent with this, about 90% of striatal neurons express DARPP-32, a MSN marker, in our experimental conditions. 3-NP reduced the number of DARPP-32-positive cells by about 30% compared with control. This reduction ratio by 3-NP is higher than the overall reduction rate assessed by the Nissl staining method (about 40% compared with control). Thus, striatal neurons that are sensitive to 3-NP were mostly MSNs.

Three lines of evidence in the present study support the hypothesis that activation of cell cycle proteins in post-mitotic neurons triggers a cell cycle reentry mechanism that leads to cell death (32, 47, 48). First, p27 level was decreased by 3-NP treatment in striatal neurons, and reduction of p27 by p27 siRNA induced cell death. Second, Rb phosphorylation was increased by 3-NP or by p27 siRNA in striatal neurons. These results were reproduced in striatum *in vivo* by 3-NP injection. Third, pharmacological CDK inhibitors protected striatal neurons against 3-NP neurotoxicity. p27 is a CDK inhibitor playing a pivotal role in cell cycle arrest at G_1/S phase, and Rb phosphorylation is a marker for cell cycle progression to late G_1 phase. Thus, findings in the current study suggest that 3-NP induces cell cycle progression in striatal neurons, which is positively associated with the cell death mechanism. This is the first report that revealed the involvement of elevated cell cycle activity in cell death of striatum.

In contrast to striatum, no evidence of increased cell cycle activity was detected in cerebral cortex exposed to 3-NP. Although previous researches that revealed the association of the cell cycle mechanism in neurotoxicity used multiple neurons (*e.g.* PC12 cells, sympathetic neurons (9), cortical neurons (11), and cerebellar granule neurons (49)), no study paid attention to the regional differences of neurons. Here we first noticed that the involvement of elevated cell cycle activity in cell death is dependent on neuronal cell types. The observations suggest that different molecular machineries are working in the neuronal cell death of striatum and cerebral cortex following 3-NP treatment. The difference in severity of cell death between striatal and cortical neurons in our data may be related to this differential molecular mechanism.

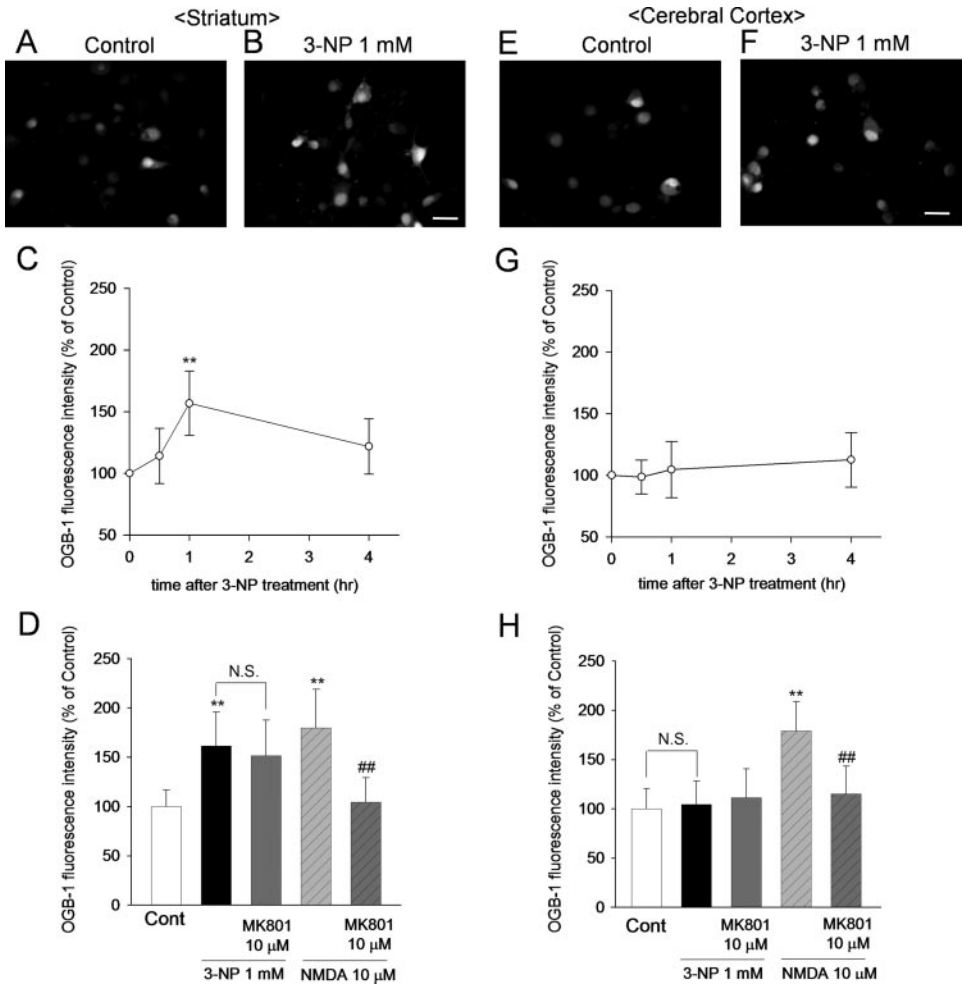

FIGURE 9. **3-NP induces an elevation of somatic Ca^{2+} in striatal but not in cortical neurons.** *A*, *B*, *E*, and *F*, representative photograph obtained from cultured striatal (*A* and *B*) and cortical (*E* and *F*) neurons bolus-loaded with OGB-1. *A* and *E*, control culture. *B* and *F*, culture exposed to 1 mM 3-NP for 1 h. *Scale bar*, 20 μm. *C* and *G*, time course of OGB-1 fluorescence intensity in the soma area of striatal (*C*) and cortical (*G*) neurons at 30 min, 1 h, and 4 h after 3-NP treatment. 3-NP induced an elevation of OGB-1 fluorescence intensity in the somata of striatal but not in cortical neurons. The results are presented as a percentage of control and represent the means ± S.E. of 168–185 neurons from three or four independent experiments. **, $p < 0.01$ *versus* control; Tukey's test. *D* and *H*, pharmacological data of OGB-1 fluorescence intensity in striatal (*D*) and cortical (*H*) neurons at 1 h after 3-NP treatment. The NMDA receptor antagonist MK801 did not block 3-NP-induced elevation of OGB-1 fluorescence in striatal neurons. In both cultures, NMDA induced an increase in OGB-1 fluorescence, which was prevented by MK801. The results are presented as a percentage of control and represent the means ± S.E. of 162–263 neurons from two independent experiments. *Cont*, control; *N.S.*, not significant. **, $p < 0.01$ *versus* control. ##, $p < 0.01$ *versus* NMDA; Tukey's test.

What causes the differential molecular machineries in 3-NP toxicity between striatal and cortical neurons? We observed the elevation of somatic Ca^{2+} and activation of the Ca^{2+}-activated protease calpain by 3-NP treatment in striatal neurons. Calpain inhibitors (*i.e.* ALLN, MDL28170, and PD150606) displayed significant neuroprotective effects against 3-NP toxicity. In contrast to these observations in striatal neurons, 3-NP did not induce any changes in somatic Ca^{2+} or calpain activity; nor did calpain inhibitors have protective effects against 3-NP toxicity in cortical neurons. These findings are consistent with observations of other groups *in vivo* (34, 50) and *in vitro* (22, 24, 51). This regional difference in Ca^{2+} dynamics may be caused by the lower intrinsic ability of striatal neurons to regulate cytosolic Ca^{2+} than cortical neurons. This hypothesis is supported by another study demonstrating that striatal mitochondria are more vulnerable to Ca^{2+}-induced permeability transition than cortical mitochondria (52). The vulnerability of striatal mitochondria to Ca^{2+} may facilitate somatic Ca^{2+} rises and a preferential activation of calpain in striatal neurons exposed to 3-NP.

We examined the molecular mechanism of the striatum-specific elevated cell cycle activity in 3-NP-induced neurotoxicity. Our previous work showed that calpain activation is required for p27 down-regulation in glutamate toxicity and that calpain(s) degrade(s) p27 (23). Moreover, we showed that p27 siRNA reduced neuronal viability (29). In the present study, we observed that p27 down-regulation induced by 3-NP in striatal neurons was abrogated by calpain inhibitors, ALLN, MDL28170, and PD150606. *In vitro* experiments using cell lysates from striatal neurons revealed that the expression level of p27 was decreased by incubation with exogenous calpain 1, which was suppressed by calpain inhibitors. The same results were obtained using cell lysates from cortical neurons or GST-p27 recombinant protein (23). Furthermore, these calpain inhibitors protected striatal neurons from the 3-NP toxicity. These results suggest that activated calpain(s) degrade(s) p27, which may induce cell cycle progression and lead to cell death in striatal neurons in 3-NP toxicity. Nonpharmacological experiments (*i.e.* overexpression of calpastatin, endogenous calpain inhibitor, or dominant negative CDK) on cell death by 3-NP) will strengthen our notion.

Protein degradation of p27 by ubiquitin-proteasome pathway has been investigated previously (35). However, lactacystin, an inhibitor of the ubiquitin-proteasome pathway, did not suppress p27 down-regulation by 3-NP in striatal neurons. Moreover, this drug had no effect on p27 degradation in neuronal cell lysates incubated with exogenous calpain 1. These results suggest that the ubiquitin-proteasome pathway is not involved in regulation of p27 expression level by 3-NP in striatal neurons. This difference may depend on the cell types (*e.g.* proliferating cells or terminally differentiated neurons as in our experiment).

The protective efficacies of either CDK inhibitors or calpain inhibitors against 3-NP toxicity were partial in striatal neurons. In contrast, co-treatment of CDK inhibitors and NMDA receptor antagonist MK801 exerted a complete neuroprotective

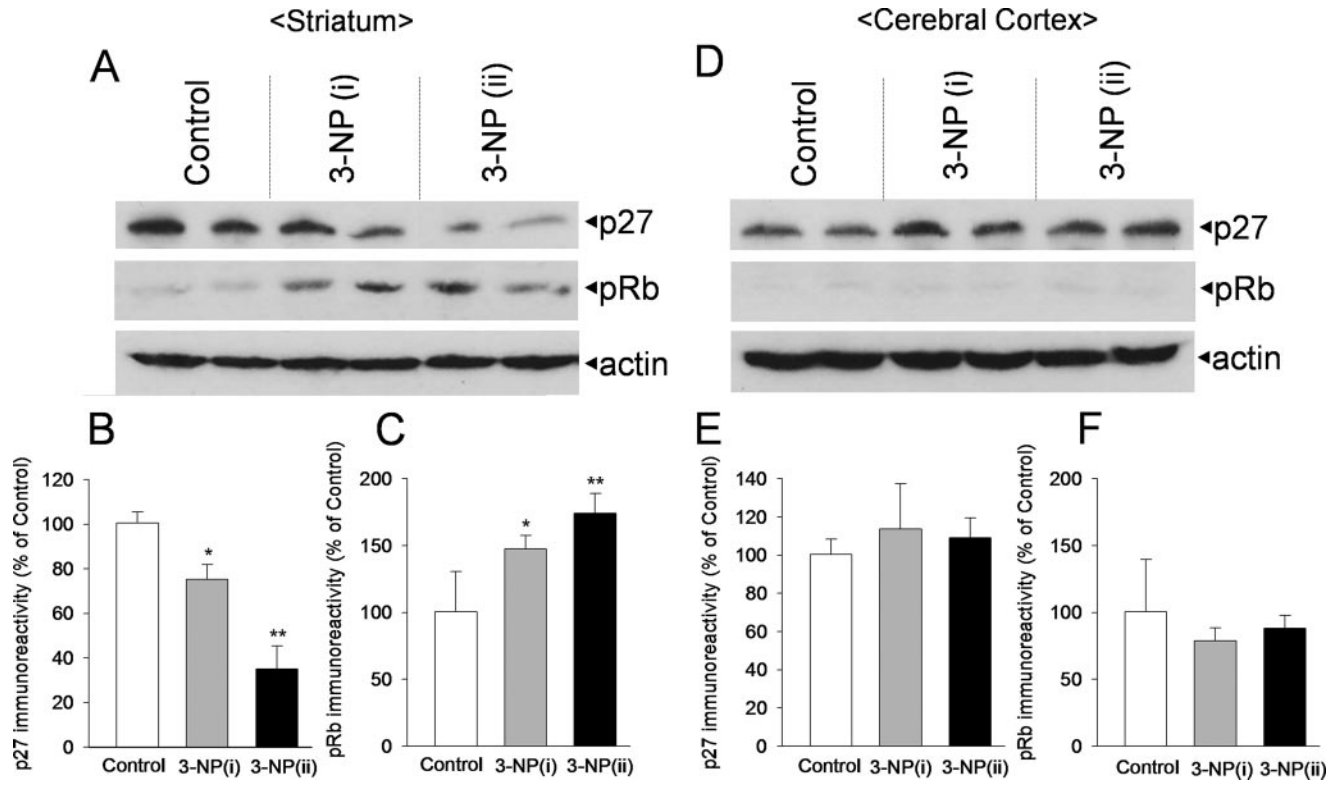

FIGURE 10. **3-NP induces striatum-specific cell cycle progression *in vivo*.** *A* and *D*, representative immunoblots of p27 and phospho-Rb (*pRb*) by 3-NP injection in striatum (*A*) and cerebral cortex (*D*). The band represents the result in different two rats in same experiment. *3-NP* (*i*) and *3-NP* (*ii*) correspond to the result of the 3-NP injection protocol: *i*, 10 mg/kg 3-NP injection intraperitoneally once every 4 days for 3 weeks; *ii*, 7.5 mg/kg 3-NP injection intraperitoneally twice daily for 5 days. Actin served as an internal control. *B* and *E*, 3-NP injection induced down-regulation of p27 in striatum (*B*) but no change in cerebral cortex (*E*). The pixel intensity of the p27 bands obtained in each experiment was calculated as described under "Materials and Methods." The results are presented as a percentage of control and represent the means ± S.E. of 3–5 different animals from two independent experiments. *, $p < 0.05$; **, $p < 0.01$ *versus* control; Tukey's test. *C* and *F*, 3-NP injection induced Rb phosphorylation in striatum (*C*) but no change in cerebral cortex (*F*). The pixel intensity of the phospho-Rb bands obtained in each experiment was calculated as described under "Materials and Methods." The results are presented as a percentage of control and represent the means ± S.E. of three or four different animals from two independent experiments.

effect against 3-NP toxicity in striatal neurons. More interestingly, singular treatment of MK801 fully rescued cortical neurons from cell death induced by 3-NP. There are controversies on the relationship between 3-NP neurotoxicity and NMDA receptor activity. Other reports (45) and the current study showed that MK801 prevented neuronal cell death induced by 3-NP. However, another study reported that MK801 failed to prevent cell death by 3-NP treatment in cultured hippocampal neurons (53). The possible cause for the discrepancy may be related to the types of cell death. MK801 attenuates necrotic but not apoptotic cell death induced by 3-NP treatment (53). Park *et al.* (54) proposed a model in which 3-NP activates interrelated necrotic (involving excitotoxicity) and apoptotic (involving cell cycle activity) pathways. It is possible to assume that we observed both necrotic and apoptotic cell death by 3-NP in striatal neurons but only necrotic cell death in cortical neurons. The present results suggest that NMDA receptor activity is commonly (partly in striatum and fully in cerebral cortex) involved in 3-NP neurotoxicity.

The elevation of calpain activity by 3-NP treatment in striatal neurons was not abrogated by MK801, suggesting that calpain activation induced by 3-NP occurred independently of the NMDA receptor. This result contrasts with previous reports that calpain activity is up-regulated by NMDA receptor in glutamate-induced neuronal damage (55, 56) and that MK801 decreased 3-NP-induced calpain elevation in cultured hippocampal neurons (57). Several explanations are plausible for the discrepancies. First, the NMDA receptor may not be sensitive to Ca^{2+} up-regulation by 3-NP in striatum. Previous evidence in striatum suggested that 3-NP enhances glutamate-induced Ca^{2+} deregulation and calpain activation independent of NMDA receptor (58). Second, calpain is activated not only by an increase in intracellular Ca^{2+} but also by other signal transduction pathways (59). Previous reports demonstrated that 3-NP-induced neurodegeneration is mediated by c-Jun in striatum (60) and mitogen-activated kinase in hippocampus (61). These pathways may be involved in 3-NP-induced calpain activation in the current study.

In both striatal and cortical neurons, caspase-3 inhibitor Z-DEVD-FMK did not protect against neuronal cell death by 3-NP treatment. Other studies showed that constant systemic infusion of 3-NP does not activate caspase-3 activity despite the neurodegeneration primarily in the striatum (34). These results suggest that 3-NP does not require an activation of caspase-3 activity to produce striatal degeneration both *in vivo* and *in vitro*.

3-NP treatment has been employed to induce an HD-like state in animals. Indeed, clinical manifestation similar to HD (*i.e.* striatal degeneration and motor deficits) is induced after 3-NP administration in rats (26). The activity of mitochondrial

succinate dehydrogenase, which is inhibited by 3-NP treatment in animals, is reduced in striatum of patients with HD (19, 20). Moreover, NMDA receptor and calpain activity, which were involved in 3-NP neurotoxicity in the current study, play key roles in HD pathogenesis (62, 63). Altogether, the present study not only revealed the mechanism of 3-NP neurotoxicity but also gave clues to explore the therapeutic strategy for HD.

In conclusion, the present results suggest that both distinct and common mechanisms are operating in striatal and cortical neurons submitted to 3-NP incubation. In the striatum, both elevated cell cycle activity via calpain-mediated p27 down-regulation and NMDA receptor activity are cooperatively involved in neuronal cell death. In contrast, only NMDA receptor activity is involved in cerebral cortex. Such intrinsic differences are of particular interest to further understand the mechanism of region-selective vulnerability in the central nervous system and human disease representing a striatal dominant phenotype of neurodegeneration and to design future neuroprotective therapies for these diseases.

Acknowledgment—We thank Takuya Sasaki for technical support in Ca^{2+} imaging.

REFERENCES

1. Stefanis, L., Burke, R. E., and Greene, L. A. (1997) *Curr. Opin. Neurol.* **10,** 299–305
2. Sherr, C. J., and Roberts, J. M. (1995) *Genes Dev.* **9,** 1149–1163
3. Freeman, R. S., Estus, S., and Johnson, E. M. (1994) *Neuron* **12,** 343–355
4. Padmanabhan, J., Park, D. S., Greene, L. A., and Shelanski, M. L. (1999) *J. Neurosci.* **19,** 8747–8756
5. Timsit, S., Rivera, S., Ouaghi, P., Guischard, F., Tremblay, E., Ben Ari, Y., and Khrestchatisky, M. (1999) *Eur. J. Neurosci.* **11,** 263–278
6. Ino, H., and Chiba, T. (2001) *J. Neurosci.* **21,** 6086–6094
7. Wen, Y., Yang, S., Liu, R., and Simpkins, J. W. (2005) *FEBS Lett.* **579,** 4591–4599
8. Farinelli, S. E., and Greene, L. A. (1996) *J. Neurosci.* **16,** 1150–1162
9. Park, D. S., Farinelli, S. E., and Greene, L. A. (1996) *J. Biol. Chem.* **271,** 8161–8169
10. Park, D. S., Levine, B., Ferrari, G., and Greene, L. A. (1997) *J. Neurosci.* **17,** 8975–8983
11. Park, D. S., Morris, E. J., Padmanabhan, J., Shelanski, M. L., Geller, H. M., and Greene, L. A. (1998) *J. Cell Biol.* **143,** 457–467
12. Rideout, H. J., Wang, Q. H., Park, D. S., and Stefanis, L. (2003) *J. Neurosci.* **23,** 1237–1245
13. Rashidian, J., Iyirhiaro, G., Aleyasin, H., Rios, M., Vincent, I., Callaghan, S., Bland, R. J., Slack, R. S., During, M. J., and Park, D. S. (2005) *Proc. Natl. Acad. Sci. U. S. A.* **102,** 14080–14085
14. Brouillet, E., Jacquard, C., Bizat, N., and Blum, D. (2005) *J. Neurochem.* **95,** 1521–1540
15. Brouillet, E., Guyot, M. C., Mittoux, V., Altairac, S., Conde, F., Palfi, S., and Hantraye, P. (1998) *J. Neurochem.* **70,** 794–805
16. Beal, M. F., Brouillet, E., Jenkins, B. G., Ferrante, R. J., Kowall, N. W., Miller, J. M., Storey, E., Srivastava, R., Rosen, B. R., and Hyman, B. T. (1993) *J. Neurosci.* **13,** 4181–4192
17. Wűllner, U., Young, A. B., Penney, J. B., and Beal, M. F. (1994) *J. Neurochem.* **63,** 1772–1781
18. Brouillet, E., Hantraye, P., Ferrante, R. J., Dolan, R., Leroywillig, A., Kowall, N. W., and Beal, M. F. (1995) *Proc. Natl. Acad. Sci. U. S. A.* **92,** 7105–7109
19. Browne, S. E., Bowling, A. C., MacGarvey, U., Baik, M. J., Berger, S. C., Muqit, M. M., Bird, E. D., and Beal, M. F. (1997) *Ann. Neurol.* **41,** 646–653
20. Gu, M., Gash, M. T., Mann, V. M., Javoy-Agid, F., Cooper, J. M., and Schapira, A. H. (1996) *Ann. Neurol.* **39,** 385–389
21. Benchoua, A., Trioulier, Y., Zala, D., Gaillard, M.-C., Lefort, N., Dufour, N., Saudou, F., Elalouf, J.-M., Hirsch, E., Hantraye, P., Deglon, N., and Brouillet, E. (2006) *Mol. Biol. Cell* **17,** 1652–1663
22. Galas, M. C., Bizat, N., Cuvelier, L., Bantubungi, K., Brouillet, E., Schiffmann, S. N., and Blum, D. (2004) *Neurobiol. Dis.* **15,** 152–159
23. Akashiba, H., Matsuki, N., and Nishiyama, N. (2006) *J. Neurochem.* **99,** 733–744
24. Behrens, M. I., Koh, J., Canzoniero, L. M. T., Sensi, S. L., Csernansky, C. A., and Choi, D. W. (1995) *Neuroreport* **6,** 545–548
25. Okuda, S., Nishiyama, N., Saito, H., and Katsuki, H. (1996) *Proc. Natl. Acad. Sci. U. S. A.* **93,** 12553–12558
26. Borlongan, C. V., Koutouzis, T. K., Randall, T. S., Freeman, T. B., Cahill, D. W., and Sanberg, P. R. (1995) *Brain. Res. Bull.* **36,** 549–556
27. Guyot, M.-C., Hantraye, P., Dolan, R., Palfi, S., Maziere, M., and Brouillet, E. (1997) *Neuroscience* **79,** 45–56
28. Abe, K., and Matsuki, N. (2000) *Neurosci. Res.* **38,** 325–329
29. Akashiba, H., Matsuki, N., and Nishiyama, N. (2006) *Cell. Mol. Life. Sci.* **63,** 2397–2404
30. Sasaki, T., Matsuki, N., and Ikegaya, Y. (2007) *J. Neurosci.* **27,** 517–528
31. Bogush, A., Pedrini, S., Pelta-Heller, J., Chan, T., Yang, Q., Mao, Z., Sluzas, E., Gieringer, T., and Ehrlich, M. E. (2007) *J. Biol. Chem.* **282,** 7352–7359
32. Liu, D. X., and Greene, L. A. (2001) *Cell Tissue Res.* **305,** 217–228
33. Beal, M. F. (1992) *Ann. Neurol.* **31,** 119–130
34. Bizat, N., Hermel, J. M., Boyer, F., Jacquard, C., Creminon, C., Ouary, S., Escartin, C., Hantraye, P., Krajewski, S., and Brouillet, E. (2003) *J. Neurosci.* **23,** 5020–5030
35. Pagano, M., Tam, S. W., Theodoras, A. M., Beerromero, P., Delsal, G., Chau, V., Yew, P. R., Draetta, G. F., and Rolfe, M. (1995) *Science* **269,** 682–685
36. Goll, D. E., Thompson, V. F., Li, H. Q., Wei, W., and Cong, J. Y. (2003) *Physiol. Rev.* **83,** 731–801
37. Hamakubo, T., Kannagi, R., Murachi, T., and Matus, A. (1986) *J. Neurosci.* **6,** 3103–3111
38. Saido, T. C., Sorimachi, H., and Suzuki, K. (1994) *FASEB J.* **8,** 814–822
39. Brecht, S., Gelderblom, M., Srinivasan, A., Mielke, K., Dityateva, G., and Herdegen, T. (2001) *Mol. Brain. Res.* **94,** 25–34
40. Tenneti, L., and Lipton, S. A. (2000) *J. Neurochem.* **74,** 134–142
41. Gould, D. H., and Gustine, D. L. (1982) *Neuropathol. Appl. Neurobiol.* **8,** 377–393
42. Gould, D. H., Wilson, M. P., and Hamar, D. W. (1985) *Toxicol. Lett.* **27,** 83–89
43. Brouillet, E., Jenkins, B. G., Hyman, B. T., Ferrante, R. J., Kowall, N. W., Srivastava, R., Roy, D. S., Rosen, B. R., and Beal, M. F. (1993) *J. Neurochem.* **60,** 356–359
44. Fink, S. L., Ho, D. Y., and Sapolsky, R. M. (1996) *Exp. Neurol.* **138,** 298–304
45. Kim, G. W., Copin, J. C., Kawase, M., Chen, S. F., Sato, S., Gobbel, G. T., and Chan, P. H. (2000) *J. Cereb. Blood Flow Metab.* **20,** 119–129
46. Ouimet, C. C., Langley-Gullion, K. C., and Greengard, P. (1998) *Brain. Res.* **808,** 8–12
47. Becker, E. B. E., and Bonni, A. (2004) *Prog. Neurobiol.* **72,** 1–25
48. Copani, A., Uberti, D., Sortino, M. A., Bruno, V., Nicoletti, F., and Memo, M. (2001) *Trends. Neurosci.* **24,** 25–31
49. Verdaguer, E., Jorda, E. G., Canudas, A. M., Jimenez, A., Pubill, D., Escubedo, E., Camarasa, J., Pallas, M., and Camins, A. (2004) *Neurochem. Int.* **44,** 251–261
50. Bizat, N., Galas, M. C., Jacquard, C., Boyer, F., Hermel, J. M., Schiffmann, S. N., Hantraye, P., Blum, D., and Brouillet, E. (2005) *Neuropharmacology* **49,** 695–702
51. Nasr, P., Gursahani, H. I., Pang, Z., Bondada, V., Lee, J. W., Hadley, R. W., and Geddes, J. W. (2003) *Neurochem. Int.* **43,** 89–99
52. Brustovetsky, N., Brustovetsky, T., Purl, K. J., Capano, M., Crompton, M., and Dubinsky, J. M. (2003) *J. Neurosci.* **23,** 4858–4867
53. Pang, Z., and Geddes, J. W. (1997) *J. Neurosci.* **17,** 3064–3073
54. Park, D. S., Obeidat, A., Giovanni, A., and Greene, L. A. (2000) *Neurobiol. Aging* **21,** 771–781
55. Siman, R., Noszek, J. C., and Kegerise, C. (1989) *J. Neurosci.* **9,** 1579–1590
56. Adamec, E., Beermann, M. L., and Nixon, R. A. (1998) *Mol. Brain. Res.* **54,** 35–48

57. Pang, Z., Bondada, V., Sengoku, T., Siman, R., and Geddes, J. W. (2003) *J. Neuropathol. Exp. Neurol.* **62,** 633–643
58. Jacquard, C., Trioulier, Y., Cosker, F., Escartin, C., Bizat, N., Hantraye, P., Cancela, J. M., Bonvento, G., and Brouillet, E. (2006) *FASEB J.* **20,** E245–E259
59. Sato, K., and Kawashima, S. (2001) *Biol. Chem.* **382,** 743–751
60. Garcia, M., Vanhoutte, P., Pages, C., Besson, M. J., Brouillet, E., and Caboche, J. (2002) *J. Neurosci.* **22,** 2174–2184
61. Sugino, T., Nozaki, K., and Hashimoto, N. (2000) *Neurosci. Lett.* **278,** 101–104
62. Cepeda, C., Ariano, M. A., Calvert, C. R., Flores-Hernandez, J., Chandler, S. H., Leavitt, B. R., Hayden, M. R., and Levine, M. S. (2001) *J. Neurosci. Res.* **66,** 525–539
63. Gafni, J., and Ellerby, L. M. (2002) *J. Neurosci.* **22,** 4842–4849